*J Toxicol Pathol 2019; 32: 155–164*

**Original Article**

# Effects of astragalus injection on different stages of early hepatocarcinogenesis in a two-stage hepatocarcinogenesis model using rats

Qian Tang[1], Mei Zhang[1], Zexuan Hong[1], Yao Chen[1], Pan Wang[1], Jian Wang[1], Zili Wang[1], Rendong Fang[1], and Meilan Jin[1]*

[1] Laboratory of Veterinary Pathology, Department of Veterinary Medicine, College of Animal Science and Technology, Southwest University, 1-13-4 Hongyuhuayuan, No. 196 Beinan Road, BeiBei District, Chongqing 400700, P.R. China

**Abstract:** To clarify the suppressive effects of astragalus injection (AI) on different stages of early hepatocarcinogenesis induced by weak promotion, SD rats initiated with a single intraperitoneal (i.p.) injection of *N*-diethylnitrosamine (DEN) at 200 mg/kg body weight and promoted with 0.5% piperonyl butoxide (PBO) in diet were repeatedly administered AI at 5 ml/kg body weight/day in the early postinitiation (EPI) or late postinitiation (LPI) period for 2 or 8 weeks, respectively. The number and area of glutathione *S*-transferase placental form (GST-P)-immunoreactive $^{(+)}$ foci tended to increase in the DEN+PBO group compared with the DEN-alone group. Among the PBO-promoted groups, number and area of GST-P$^+$ foci did not visibly change in the DEN+PBO+AI-EPI group compared with the DEN+PBO group. In contrast, number and area of GST-P$^+$ foci tended to decrease in the DEN+PBO+AI-LPI group compared with the DEN+PBO group. Number of Ki67$^+$ cells was increased in the DEN+PBO group compared with the DEN-alone group and was decreased in both AI-administered groups compared with the DEN+PBO group. Gene expression analysis revealed that the DEN+PBO+AI-LPI group showed increased transcript levels of *Ccne1*, *Cdkn1b*, *Rb1*, *Bax*, *Bcl2*, *Casp3,* and *Casp9* compared with the DEN+PBO group; however, the DEN+PBO+AI-EPI group did not show changes in the transcript levels of any genes examined compared with the DEN+PBO. These results suggest that AI administration during the LPI period caused weak suppression of hepatocarcinogenesis under weak promotion with a low PBO dose by the mechanism involving facilitation of cell cycle suppression causing G1/S arrest and apoptosis via the mitochondrial pathway. In addition, the results suggest that AI administration during the EPI period has no effect on weakly promoted hepatocarcinogenesis. (DOI: 10.1293/tox.2019-0006; J Toxicol Pathol 2019; 32: 155–164)

**Key words:** astragalus injection, two-stage hepatocarcinogenesis, apoptosis, cell proliferation activity, cell cycle

## Introduction

Astragalus is the dried root of Astragalus membranaceus (Fisch.) Bge. Var. Mongholicus (Bge.) Hsia or Astragalus membranaceus (Fisch.) Bge., also known as Astragali Radix or Huangqi, and it has been widely used as a traditional Chinese medicine for treatment of various diseases for more than 2000 years. According to the information from traditional Chinese medicine, astragalus has effects that tonify Qi (Qi refers to the driving force for maintaining normal functions of the human body) and lifting Yang (Yang mainly refers to body function), strengthening the exterior (this is not body's exterior) and reducing sweat, as well as promoting the secretion of saliva or body fluids. Astragalus comprises flavonoids, saponins, polysaccharides, various amino acids, and trace elements[1, 2]. Previous studies have shown that astragalus increases telomerase activity and has antioxidant, anti-inflammatory, immune-regulatory, anticancer, hypolipidemic, antihyperglycemic, hepatoprotective, expectorant, and diuretic effects[3–8].

Astragalus injection (AI) is prepared from astragalus by the following steps: water extraction, alcohol precipitation, alkali addition, and adsorption of pigments by activated carbon. Purified AI contains 18 active ingredients, including pratensein 7-*O*-glucopyranoside, calycosin-7-*O*-β-D-glucoside, astragaloside I, astragalin, 4′-hyadroxysoflavone-7-*O*-β D-glucoside, pratensein, pterocarpane-3-glucoside, methylnissolin-3-*O*-glucoside, isomucronulatol, isorhamnetin, isorhamnetin-3-*O*-gentiobioside, medicarpin, 6″-acetylcalycosin-7D-glucoside, astragaloside V, astragaloside VI, astragaloside VII, astragaloside IV, and lrioresinol B[9]. Studies on the anticancer effects of astragalus and its main components have been performed, and abundant evidence has

Received: 17 January 2019, Accepted: 12 March 2019
Published online in J-STAGE: 15 April 2019
*Corresponding author: M Jin (e-mail: meilan0622@swu.edu.cn)

shown that astragalus and its main components inhibit cell proliferation, inhibit oxidative stress, and induce apoptosis in various cancer cells[10–12]. For example, astragalosides inhibit human colon cancer cell proliferation by inducing cell cycle arrest in the S and G2/M phases[13]. Astragalus mongholicus injection inhibits MCF-7 breast cancer cell proliferation by inducing G0/G1 and S phase arrest[14]. In addition, flavonoids from astragalus inhibit the development of breast cancer by promoting cancer cell apoptosis[12]. Astragaloside IV inhibits hepatic stellate cell activation by inhibiting oxidative stress and associated p38 MAPK activation[15]. Furthermore, flavonoids from Astragalus complanatus induce human hepatocarcinoma cell apoptosis by increasing caspase-3, caspase-8, BAX, $P21^{CIP1/WAF1}$, and $p27^{KIP1}$ protein levels[16]. Moreover, we have found that the decoction products of Astragalus membranaceus have a certain inhibitory effect on the promotion stage of early hepatocarcinogenesis in SD rats (unpublished data). Overall, these studies suggest that astragalus inhibits the development of tumors by inhibiting cell proliferation and inducing apoptosis in vitro and in vivo. However, it remains unclear if AI has the same effects on hepatocellular proliferative lesions of early hepatocarcinogenesis in animal models.

The two isomers of 4-hydroxy-5-hydroxymethyl-[1,3] dioxolan-2,6'-spirane-5',6',7',8'-tetrahydro-indolizine-3'-carbaldehyde (HDTIC)-1 and HDTIC-2 from astragali radix slow the telomere shortening rate by attenuating oxidative stress and increasing DNA repair ability in human foetal lung diploid fibroblast cells[17]. Limagne et al. reported that the active ingredients of astragalus have a repairing effect on DNA damage and that there is a close relationship between the cancerization of normal cells and DNA damage[18]. In addition, astragalus polysaccharide relieves oxidative damage induced by $H_2O_2$ by promoting APE/Ref-1 and TRX expression in damaged MRC-5 cells[19]. These studies suggest that astragalus inhibits DNA damage in cancer cells in vitro. Thus, astragalus and its main components not only relieve DNA damage but also inhibit cell proliferation of various tumor cells and induce cancer cell apoptosis. However, it remains unclear if AI has these effects on the initiation or promotion phase of early hepatocarcinogenesis in SD rats.

The present study was performed to examine the modifying effect of a clinically applied level of AI on different stages of early hepatocarcinogenesis, consisting of the early postinitiation (EPI) period showing transition from extensive liver cell injury after strong genotoxic stimulation by a tumor-initiation treatment to liver cell regeneration and the late postinitiation (LPI) period showing selective proliferation of initiated cells, using a rat two-stage hepatocarcinogenesis model. For this purpose, we selected two different postinitiation periods, i.e., the EPI period comprising the 2 weeks just after the tumor initiation treatment, showing transition from extensive liver cell injury by initiation treatment to liver cell regeneration, and the LPI period for following the 8 weeks following the EPI period. Because the present study was aimed at investigating the inhibitory effect of a clinically applied level of AI, we decided to create a cellular environment for tumor promotion to initiate the carcinogenic process as slowly as possible to mimic clinically relevant situations.

## Materials and Methods

### *Chemicals*

AI was purchased from Chiatai Qingchunbao Pharmaceutical Co., Ltd. (Hangzhou, China). *N*-diethylnitrosamine (DEN) was purchased from TCI Chemicals Co., Ltd. (Shanghai, China). Piperonyl butoxide (PBO) was purchased from Aladdin® (Shanghai, China). Anti-glutathione *S*-transferase placental form (GST-P) pAb was purchased from Medical and Biological Laboratories Co., Ltd. (1:1000; Nagoya, Japan). Anti-Ki67 antibody [SP6] was purchased from Abcam (1:500; Shanghai, China). The real-time PCR primers listed in Table 1 were designed and synthesized by Thermo Fisher Scientific (Chengdu, China).

### *Experimental design*

The protocol for this study was approved by the Animal Care and Utilization Committee of Southwest University (Chongqing, China). A total of 40 male SD rats aged 5 weeks were purchased from Chongqing Academy of Chinese Materia Medica (Chongqing, China). SD rats were housed in polycarbonate cages (3 or 4 rats per cage) with hardwood chips for bedding in a conventional animal facility and were maintained under conditions of controlled temperature (22 ± 2°C), humidity (55 ± 5%), ventilation (12 air changes per hour), and lighting (12 h light/dark cycle). SD rats were allowed free access to a basal diet (Ensiveier, Co., Chongqing, China) and tap water.

After a 1 week acclimatization period, animals were subjected to a tumor-initiation treatment, promotion treatment, and partial hepatectomy following the protocol of a medium-term liver carcinogenesis bioassay[20]. Forty five-week-old male SD rats were divided randomly into the following 4 groups with 10 animals per group: DEN-alone, DEN+PBO, DEN+PBO+AI-EPI, and DEN+PBO+AI-LPI (Fig. 1). All animals received an intraperitoneal (i.p.) injection of DEN at a dose of 200 mg/kg body weight, and all animals in the DEN+PBO, DEN+PBO+AI-EPI, and DEN+PBO+AI-LPI groups were fed a diet containing 0.5% PBO for 8 weeks starting 2 weeks after DEN initiation[21]. To enhance hepatocellular proliferation, all animals were subjected to a two-thirds partial hepatectomy 1 week after PBO treatment. To investigate the suppressive effects of AI on early hepatocarcinogenesis in rats, animals of the DEN+PBO+AI-EPI group received i.p. injections of AI at a dose of 5 ml/kg every day for 2 weeks after DEN treatment. In addition, animals of the DEN+PBO+AI-LPI group received i.p. injections of AI at a dose of 5 ml/kg every day for 8 weeks with PBO treatment. Three rats died due to an insufficiency caused by hepatectomy treatment. Body weight and food consumption were measured once a week. At the end of the experiment, rats were euthanized by ether anesthesia, and livers were excised and weighed. Sliced liver

**Table 1.** Sequence of Primers Used for Real-time Reverse Transcription-polymerase Chain Reaction (RT-PCR) Analysis

| Accession no. | Gene description | Gene symbol | Forward primer sequence (5'→3') | Reverse primer sequence (5'→3') |
|---|---|---|---|---|
| Cell cycle-related genes | | | | |
| NM_022381 | Proliferating cell nuclear antigen | *Pcna* | AGGGCTGAAG ATAATGCTGA TACC | TCCTGTTCTG GGATTCCAAG TT |
| NM_171992 | G1/S-specific cyclin-D1 | *Ccnd1* | CGTGGCCTCT AAGATGAAGG A | TCGGGCCGGA TAGAGTTGT |
| NM_001100821 | G1/S-specific cyclin-E1 | *Ccne1* | AAGTGGCCTAC GTCAACGACA | ATCAACTCCA ACGAGGAAAA ATG |
| NM_199501 | Cyclin-dependent kinase 2 | *Cdk2* | TTGACGGGAG AAGTTGTGG C | CTTGACGATG TTAGGGTGAT TGAG |
| NM_053593 | Cyclin-dependent kinase 4 | *Cdk4* | TACAAAGCCC GAGATCCCCA | GACATCCATC AGCCGTACAA CA |
| NM_031762 | Cyclin-dependent kinase inhibitor 1B | *Cdkn1b* | CCCGGTCAAT CATGAAGAAC TAA | CCTCTCCACC TCCTGCCACT |
| NM_017045 | Retinoblastoma 1 | *Rb1* | TTGTTCTCTC AGCCTCCCTC TC | CTGCTTGCGT CTCTGTATTT GC |
| Apoptosis-related genes | | | | |
| NM_030989 | Tumor protein p53 | *Tp53* | AGTGGGAATC TTCTGGGACG G | GCTGGGGAGA GGAGCTTGTG |
| NM_017059 | Apoptosis regulator | *Bax* | CCCGAGAGGT CTTCTTCCGT | CCAGTGTCCA GCCCATGATG |
| NM_016993 | Apoptosis regulator | *Bcl2* | CCCCTGGCAT CTTCTCCTTC | GCGACGGTAG CGACGAGAG |
| NM_012922 | Caspase 3 | *Casp3* | TTGGAACGAA CGGACCTGTG | TCCAGCTCTG TACCTCGGCA |
| NM_022277 | Caspase 8 | *Casp8* | TAACTTCCAG AAAGCGGTGC C | AGCCATCCCC AGCAGAAAGT |
| NM_031632 | Caspase 9 | *Casp9* | TTCCTCAGGG CTCAGCACAC | GCCGTGACCA TTTTCTTAGC A |
| NM_031144 | Actin, beta | *Actb* | CCCTGGCTCC TAGCACCAT | AGAGCCACCA ATCCACACAG A |

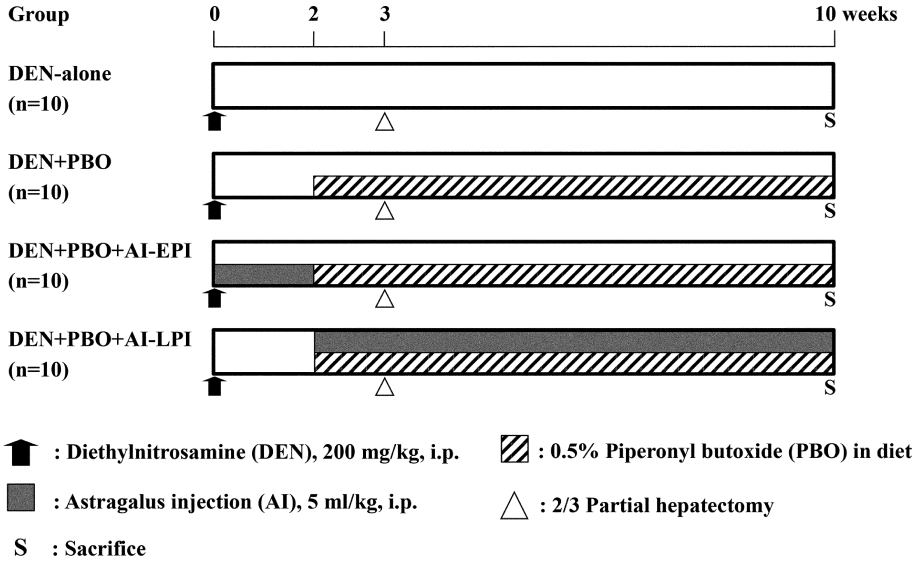


**Fig. 1.** Experimental design.

samples were fixed in 10% phosphate buffered formalin for histopathology and immunohistochemistry analyses. The remaining liver pieces were frozen in dry ice and stored at −80°C until further analysis.

*Histopathology and immunohistochemistry*

The fixed liver slices were dehydrated in graded ethanol, embedded in paraffin, sectioned, and stained with hematoxylin and eosin (HE) for histopathological examinations. Immunohistochemical staining of GST-P and Ki-67 was performed. Deparaffinized liver sections were treated with 0.3% $H_2O_2$ in methanol for 30 min to block endogenous peroxidase, and tissue sections were boiled in 0.01 M citrate buffer for antigen retrieval (for Ki67 only) and then blocked with 1% normal goat serum (SouthernBiotech, Birmingham, AL, USA) or horse serum (Vector Laboratories, Burlingame, CA, USA) for 30 min at room temperature. Sections were then incubated overnight at 4°C with anti-GST-P pAb (1:1,000 dilution; Medical and Biological Laboratories Co., Ltd., Nagoya, Japan) or anti-Ki67 antibody (1:500 dilution, Abcam, Shanghai, China). After incubation with a biotin-conjugated secondary antibody, sections were incubated with VECTASTAIN® ABC Reagent (PK-6100, Vector Laboratories, Burlingame, CA, USA) and 3,3-diaminobenzidine (DAB; Aladdin®, Shanghai, China). All specimens were lightly counterstained with hematoxylin. The numbers and areas of GST-P-positive (GST-P$^+$) liver cell foci with a diameter ≥200 μm[22, 23], as well as total areas of liver sections, were measured using Sunny Digital microscope lab system computer software (Ningbo Sunny Instruments Co., Ltd., China). Ki67$^+$ cells were examined in a total of 30 fields at 40×10 magnification in different regions (approximately 2,000–5,000 hepatocytes in each field) per animal with the free Katikati2 software, and cells with strongly positive nuclei were considered for the Ki67$^+$ cell ratio.

*RNA isolation and quantitative real-time RT-PCR for mRNA expression*

Briefly, total RNA was isolated from four or five rats in each group using TRIzol reagent (Thermo Fisher Scientific, Walthan, MA) according to the manufacturer's instructions. Total RNA was reverse transcribed using TheromoScript Reverse Transcriptase (SuperScript III First-Strand Synthesis System; Invitrogen, Thermo Fisher Scientific, Waltham, USA). All PCR assays were performed using SYBR Green Master Mix (Applied Biosystems, Thermo Fisher Scientific, Waltham, USA) and were performed under the following conditions using a C1000-CFX96 Real-Time PCR System (Bio-Rad Laboratories, Hercules, CA, USA): 50°C for 2 min, 95°C for 10 min, and 45 cycles for 15 seconds at 95°C and 60°C for 1 min. The relative differences in gene expression were calculated using threshold cycle (*C*t) values normalized to *Actb* (endogenous control in the same sample) and then compared to a control *C*t value using the $2^{-\Delta\Delta t}$ method[24]. Data represent the average fold changes with standard deviation.

*Statistical analysis*

All data are expressed as the mean ± standard deviation. The statistical significance of differences between the DEN alone and PBO-treated group or between the DEN+PBO group and AI-treated groups was determined by Dunnett's test or Williams test. A *P*-value less than 0.05 was considered statistically significant.

## Results

*General condition and body and liver weights*

Body weight gains were suppressed in the PBO-treated rats from 2 weeks after the partial hepatectomy to the end of the experiment (data not shown). Final body weight did not change between the DEN-alone and DEN+PBO groups (Table 2). Among PBO-promoted groups, the body weight of DEN+PBO+AI-LPI animals was significantly decreased compared with that of the DEN+PBO group. Regarding the liver weights, the absolute and relative liver weights in the DEN+PBO group were significantly increased compared with those of the DEN-alone group (Table 2). Among PBO-promoted groups, the DEN+PBO+AI-LPI group showed a decreased absolute weight compared with the DEN+PBO group. No changes were observed in both absolute and relative liver weights in the DEN+PBO+AI-EPI group compared with the DEN+PBO group. No significant difference in food consumption was observed between the DEN-alone and DEN+PBO groups or between the DEN+PBO and each of the AI-treated groups (data not shown).

*Effects of AI treatment on histopathology, GST-P$^+$ foci, and cell proliferation*

Histopathological analysis showed that PBO-treated animals induced hepatocellular vacuolation, which was significantly reduced in AI-treated groups (data not shown). The number and area of GST-P$^+$ foci in the DEN+PBO group showed an increasing tendency compared with those in the DEN-alone group (Fig. 2). Among PBO-promoted groups, number and area of GST-P$^+$ foci did not visibly change in the DEN+PBO+AI-EPI group compared with the DEN+PBO group. In contrast, number and area of GST-P$^+$ foci tended to decrease in the DEN+PBO+AI-LPI group compared with the DEN+PBO group. The effect of AI on cell proliferation was evaluated by immunohistochemistry for Ki67 (Fig. 3). The number of Ki67$^+$ hepatocytes was significantly increased in the DEN+PBO group compared with the DEN-alone group and was decreased in DEN+PBO+AI-EPI and DEN+PBO+AI-LPI groups compared with the DEN+PBO group.

*Transcript level of cell cycle-related genes*

To evaluate the effect of AI treatment on the EPI and LPI phases in the two-stage hepatocarcinogenesis assay, liver tissues were subjected to real-time RT-PCR analysis. The main components of astragalus inhibit cancer cell proliferation[15]. Therefore, the mRNA expression of cell cycle checkpoint regulatory genes (*Pcna*, *Ccnd1*, *Ccne1*, *Cdk2*,

**Table 2.** Body and Liver Weights

| Group | DEN-alone | DEN+PBO | DEN+PBO+AI-EPI | DEN+PBO+AI-LPI |
|---|---|---|---|---|
| No. of animals examined | 9 | 9 | 9 | 10 |
| Final body weight (g) | 362.7 ± 60.4[a)] | 338.7 ± 26.0 | 340.0 ± 26.9 | 311.8 ± 28.7*[#] |
| Liver weight | | | | |
| Absolute weight (g) | 8.89 ± 1.60 | 11.07 ± 1.29** | 11.38 ± 1.35** | 9.95 ± 0.81[#] |
| Relative weight (g/100 g body weight) | 2.44 ± 0.11 | 3.26 ± 0.20** | 3.35 ± 0.27** | 3.20 ± 0.15** |

AI, astragalus injection; DEN, *N*-diethylnitrosamine; EPI, early postinitiation; LPI, late postinitiation; PBO, piperonyl butoxide. [a)]Mean ± SD. *$P$<0.05 vs. DEN group (Dunnett's test or Williams test). **$P$<0.01 vs. DEN group (Dunnett's test or Williams test). [#]$P$<0.05 vs. DEN+PBO group (Dunnett's test or Williams test).

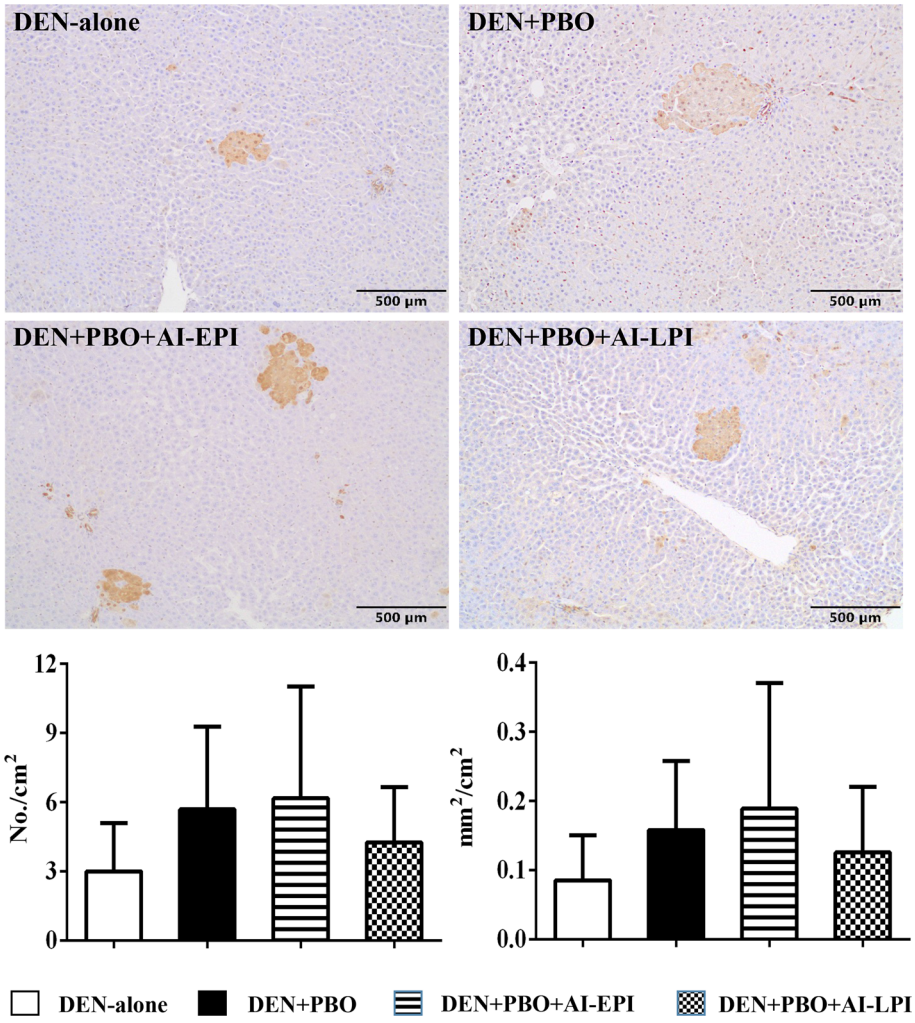


**Fig. 2.** The effect of astragalus injection (AI) on the area and number of GST-P-positive (GST-P$^+$) foci in the liver of rats given piperonyl butoxide (PBO) after *N*-diethylnitrosamine (DEN) initiation. Values are expressed as means ± SD for rats in the DEN-alone group (n=9), DEN+PBO group (n=9), DEN+PBO+AI-EPI group (n=9) and DEN+PBO+AI-LPI (n=10). EPI, early postinitiation; LPI, late postinitiation.

*Cdk4*, *Cdkn1b,* and *Rb1*) was investigated (Fig. 4). The *Pcna* mRNA expression level in the DEN+PBO group was significantly increased compared with the DEN-alone group, but the level in the AI-treated groups tended to decrease compared with the DEN+PBO group. There were no mRNA expression changes of other genes between the DEN-alone and DEN+PBO groups. Among PBO-promoted groups, mRNA expression levels of *Ccne1*, *Cdkn1b,* and *Rb1* were significantly increased in the DEN+PBO+AI-LPI group compared with the DEN+PBO group. There were no significant changes in the mRNA expression levels of *Ccnd1*, *Cdk2,* or *Cdk4* between the DEN+PBO and AI-treated groups (Fig. 4).

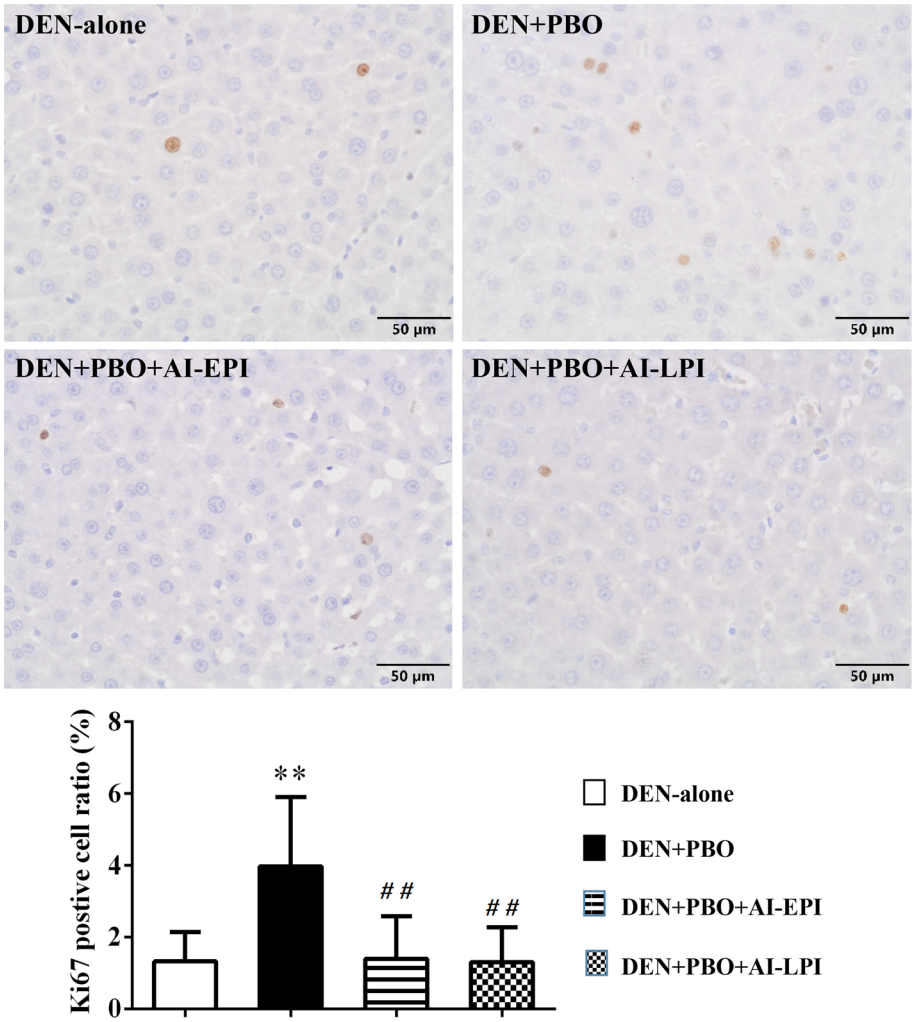


**Fig. 3.** The effect of astragalus injection (AI) on the quantitation of Ki67$^+$ cells. Values are expressed as means ± SD for rats in the DEN-alone group (n=9), DEN+PBO group (n=9), DEN+PBO+AI-EPI group (n=9) and DEN+PBO+AI-LPI (n=10). **Significantly different from the DEN-alone group by Dunnett's test or Williams test ($P$<0.01). ## Significantly different from the DEN+PBO group by Dunnett's test or Williams test ($P$<0.01). EPI, early postinitiation; LPI, late postinitiation.

*Transcript level of apoptosis-related genes*

Previous studies have shown that the main components of astragalus induce cancer cell apoptosis[13]. Therefore, mRNA expression levels of apoptosis-related genes (*Tp53*, *Bax*, *Bcl2*, *Casp3*, *Casp8,* and *Casp9*) were examined in the liver tissue (Fig. 5). The mRNA expression levels of these genes in the DEN+PBO group were not significantly changed compared with the DEN-alone group. Among PBO-promoted groups, mRNA expression levels of *Bax*, *Bcl2*, *Casp3,* and *Casp9* in the DEN+PBO+AI-LPI were significantly higher than those of the DEN+PBO group. In addition, there were no significant changes between the DEN+PBO and AI-EPI groups.

## Discussion

As tumors are characterized by dysregulation of cellular proliferation, reducing abnormal cell proliferation plays an important role in host defence and protection from cancer development[25]. Many studies have suggested that induction of cell cycle arrest, apoptosis, and anti-oxidative effects in cancer cells is a promising approach for the treatment of cancer[26–28]. Astragalus membranaceus has been used for centuries in China to treat liver diseases. In recent years, it has been reported that astragalus or its active ingredients can inhibit the proliferation of hepatoma cell lines and induce apoptosis of cancer cells[10, 29, 30]. We previously found that astragalus decoction products suppress GST-P$^+$ foci and cell proliferation activity in the early stages of hepatocarcinogenesis in SD rats (unpublished data). Therefore, it is reasonable to clarify the possibility of AI as a chemopreventive agent of hepatocellular tumors. It is also important to elucidate whether AI exerts an inhibitory effect at the early stage of hepatocarcinogenesis and also the action stage of AI during early hepatocarcinogenesis. Based on the aforementioned information of AI as a candidate therapeutic model,

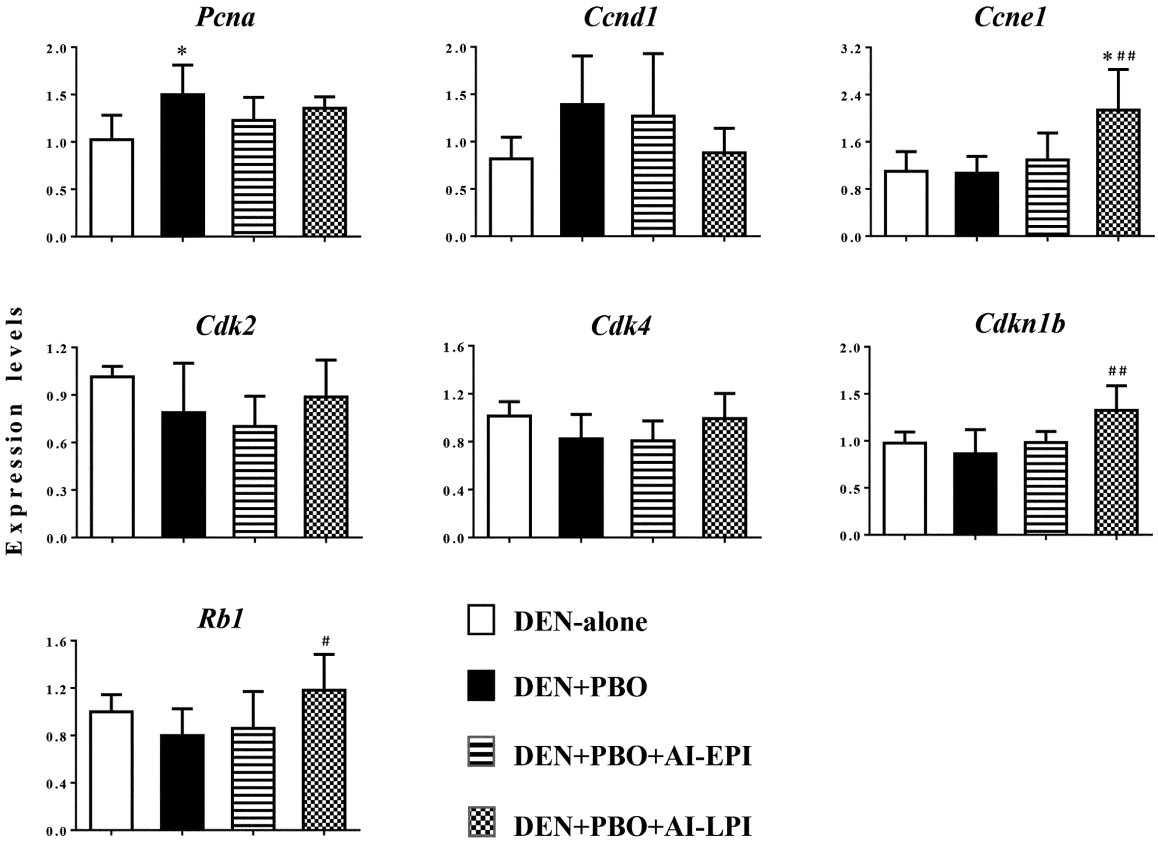


**Fig. 4.** The effect of astragalus injection (AI) on mRNA expression levels of cell cycle-related genes in the livers of SD rats given piperonyl butoxide (PBO) after *N*-diethylnitrosamine (DEN) initiation. Relative values of mRNA expression levels (normalized by *Actb*) are expressed as means ± SD. * Significantly different from the DEN group by Dunnett's test or Williams test ($P<0.05$). # Significantly different from the DEN+PBO group by Dunnett's test or Williams test ($P<0.05$). ## Significantly different from the DEN+PBO group by Dunnett's test or Williams test ($P<0.01$). EPI, early postinitiation; LPI, late postinitiation.

the present study conducted an anticancer experiment using AI, a purified product consisting of 18 active ingredients extracted from astragalus, to confirm the action stage during the postinitiation period and the suppression mechanisms of AI in the early stage of hepatocarcinogenesis in SD rats.

Flavonoids from Astragalus complanatus reduce DNA injury and mutation *in vitro*[31]. In addition, HDTIC, an isomer extracted from Astragalus membranaceus, improves DNA repair ability[17]. These results suggest that astragalus has a protective effect on DNA damage. In contrast, the rhamnocitrin 4-β-D-galactopyranoside flavonoid obtained from leaves of astragalus prevents induction of hepatocellular carcinoma accompanying suppression of the marked increase in the levels of serum marker enzymes, and it suppresses free radicals by scavenging hydroxyl radicals[32]. In addition, swainsonine, an extract from Astragalus membranaceus, significantly inhibits MHCC97-H cell growth by causing cell cycle arrest at the G0/G1 phase and inducing apoptosis[33]. In the present study, AI treatment in the LPI stage not only decreased the body weight but also weakly inhibited the number and area of GST-P$^+$ foci weakly increased by PBO promotion in early hepatocarcinogenesis. It is reported that oral administration of 1 ml/kg AI for 28 days can inhibit body weight gain of exhaustively exercised rats by enhancing the activity of metabolic enzymes[34]. In the present study, AI treatment reduced hepatocellular vacuolation, which suggested that it had an ameliorating effect on PBO-induced hepatotoxicity. Therefore, the decrease of body weight in the DEN+PBO+AI-LPI group may be due to increased metabolic activity rather than hepatocellular toxicity caused by AI, suggesting that the possibility of AI-induced toxicity to affect a tumor-promoting effect is rather low. In addition, relative liver weight in the DEN+PBO+AI-LPI group was unchanged compared with the DEN +PBO group. Therefore, a decrease in absolute liver weight may be accompanied by the body weight decrease due to increased metabolic activity.

In the present study, Ki-67 immunostaining showed that AI treatment in both the EPI and LPI periods significantly inhibited the Ki67$^+$ cell ratio. In addition, the expression levels of PCNA in both AI-treated groups tended to decrease compared with the DEN+PBO group. The Ki67 nuclear antigen is a proliferative marker and is a good indicator of the proliferative and differentiation ability of carcinoma cells[35]. These results indicated that AI has a strong inhibitory effect on cell proliferation during the early stage

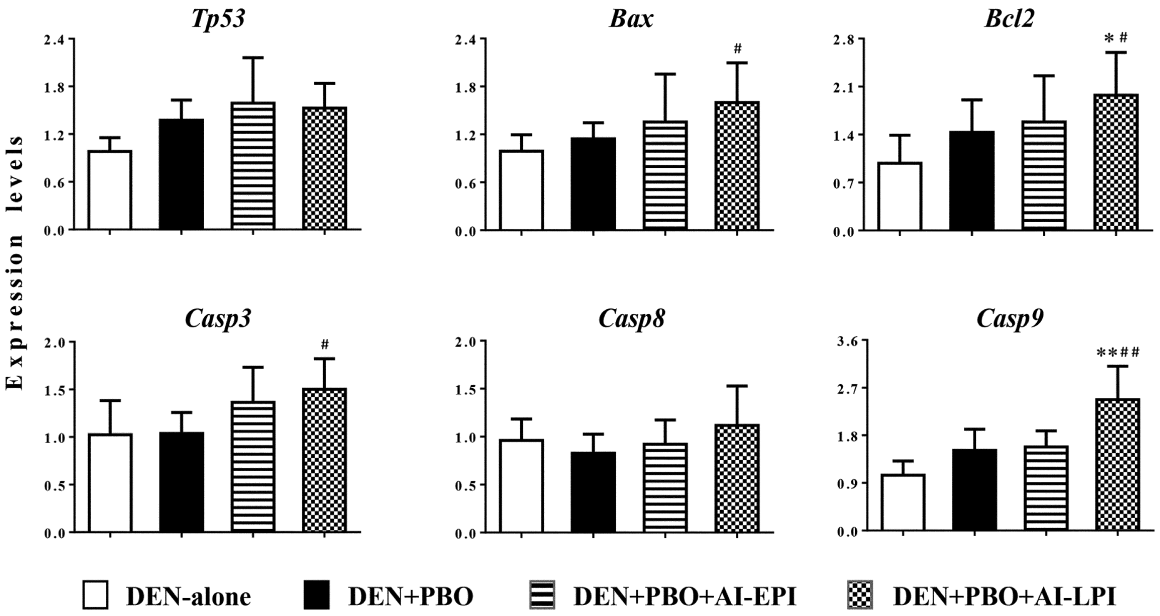


**Fig. 5.** The effect of astragalus injection (AI) on mRNA expression levels of apoptosis-related genes in the livers of SD rats given piperonyl butoxide (PBO) after *N*-diethylnitrosamine (DEN) initiation. Relative values of mRNA expression levels (normalized by *Actb*) are expressed as means ± SD. * Significantly different from the DEN group by Dunnett's test or Williams test ($P<0.05$). ** Significantly different from DEN group by Dunnett's test or Williams test ($P<0.01$). #Significantly different from the DEN+PBO group by Dunnett's test or Williams test ($P<0.05$). ##Significantly different from the DEN+PBO group by Dunnett's test or Williams test ($P<0.01$). EPI, early postinitiation; LPI, late postinitiation.

of hepatocarcinogenesis. However, we observed no influence of AI treatment during the EPI period on the area and number of GST-P$^+$ foci promoted by PBO, in contrast to the weak suppression of tumor promotion by AI during the LPI period. However, it remains unclear whether the antiproliferative effect is involved in the anticancer mechanism of AI during the LPI period. An antiproliferative effect involving the GST-P$^+$ liver cell population probably occurs as a result of AI-LPI but dose not occur in DEN-initiated cells as a result of EI-LPI. To clarify the suppression mechanism of AI on hepatocellular proliferative lesions during early hepatocarcinogenesis, further studies may be necessary on the temporal change in target cells of AI during the postinitiation period.

The present study showed that AI not only significantly inhibited the Ki67$^+$ cell ratio in the liver but also reduced the expression level of *Pcna* increased by PBO promotion. Both PCNA and Ki67 are nuclear antigens in proliferating cells, and they are essential nuclear proteins for DNA synthesis in eukaryotic cells[36, 37]. Ki67 accumulates in the late G1/S phase and rapidly degrades in the late phase of mitosis[38]. The abnormal expression of PCNA can be used to evaluate the degree of malignancy and proliferation potential of tumors, and PCNA shows different expression levels in tumors of various stages of development. The expression of PCNA begins at the S phase and reaches the highest peak at the G1 phase, but it decreases at the G2/M phase[39, 40]. Therefore, we further examined the expression levels of genes related to the cell cycle G1/S phase. As a result, we found upregulation of *Cdkn1b* (p27$^{KIP1}$), *Rb1,* and *Ccne1* in the DEN+PBO+AI-LPI group compared with the DEN+PBO group. p27$^{KIP1}$, a cell cycle inhibitor, has been demonstrated to inhibit CDK4 or CDK2 bound to cyclin D1 or cyclin E, and the upregulation of the *Cdkn1b* gene induces G1 phase arrest[41]. In addition, Rb is a tumor suppressor that negatively regulates the G1/S transition of the cell cycle, and it is present in 70% of all tumors[42, 43]. Our results suggest that AI may inhibit cell proliferation by inducing G1/S phase arrest in the promotion period during early hepatocarcinogenesis. On the other hand, cyclin E and CDK2 form a complex and can phosphorylate and inactivate Rb, resulting in E2F activation and a shortened G1 phase, thereby expelling cells into the S phase, which promotes cell proliferation[44]. However, the mRNA expression level of CDK2 was not significantly increased in the present study. This result indicated that the upregulation of cyclin E may be due to an increase in the number of cells in the G1 phase resulting from the AI-induced G1/S phase arrest due to imbalance of CDK2 and cyclin E.

In the present study, we observed that increased gene expression levels of apoptosis-related genes (*Bax*, *Bcl2*, *Casp3*, *Casp9*) were observed by real-time RT-PCR. The BCL2 protein family comprises large apoptosis regulatory proteins, and increases of the BCL2 protein family member, BAX, lead to the release of cytochrome C and other proapoptotic molecules from the intermembranous space to the cytosol, resulting in activation of downstream caspases[45]. In the mitochondrial-dependent apoptotic pathway, the

membrane potential of mitochondria decreases significantly in the early stage of apoptosis, releasing cytochrome C in mitochondria, which cooperates with caspase-9 to further activate caspase-3[46]. In addition, it has been reported that various anticancer drugs induce apoptosis by activating the caspase-9/caspase-3 pathway and increasing BCL2 protein family members in various cancer cells[47, 48]. Although there was no significant difference, the number and area of GST-P$^+$ foci in the DEN+PBO-AI-LPI group showed a tendency to decrease compared with the DEN+PBO group, suggesting that AI treatment during the LPI period contributes to facilitation of the mitochondrial-dependent apoptotic pathway in GST-P$^+$ foci. Furthermore, AI treatment inhibited the Ki-67$^+$ cell ratio increased by PBO promotion, possibly as a result of AI-induced G1/S arrest. The obtained results in the present study indicated that AI induces hepatocyte apoptosis and G1/S arrest in the LPI (promotion) period of hepatocarcinogenesis and that these effects may be closely linked to events leading to inhibition in the development of preneoplastic lesions. Further study on the temporal relationships of apoptosis, cell proliferation, and cell cycle-related molecules with GST-P$^+$ foci will be necessary to be addressed to clarify the AI-induced suppression effect on hepatocarcinogenesis.

In conclusion, the present study investigated the suppression effects of AI on different stages of early hepatocarcinogenesis initiated with DEN and promoted with PBO. The overall data suggested that AI treatment in the promotion stage of early hepatocarcinogenesis can inhibits cell proliferation activity and induces apoptosis through facilitation of G1/S phase arrest and caspase-9/3 pathway activation, leading to suppression the development of preneoplastic lesions on the promotion period. In addition, treatment with AI during the early postinitiation period can inhibit cell proliferation but cannot suppress the hepatocarcinogenesis. Further studies are necessary to clarify the potential suppression mechanism of AI in early hepatocarcinogenesis.

**Disclosure of Potential Conflicts of Interest:** We have no conflicts of interest to be declared.

**Acknowledgments:** This work was supported by the Fundamental Research Funds for the Central Universities (XDJK2016B019) and National Special Funds for Major Research Instrumentation Development (SWU114028).

## References

1. Li X, Qu L, Dong Y, Han L, Liu E, Fang S, Zhang Y, and Wang T. A review of recent research progress on the astragalus genus. Molecules. **19**: 18850–18880. 2014. [Medline] [CrossRef]
2. Jin M, Zhao K, Huang Q, and Shang P. Structural features and biological activities of the polysaccharides from Astragalus membranaceus. Int J Biol Macromol. **64**: 257–266. 2014. [Medline] [CrossRef]
3. Ma JW, Qiao ZY, and Xiang X. Aqueous extract of Astragalus mongholicus ameliorates high cholesterol diet induced oxidative injury in experimental rat models. J Med Plants Res. **5**: 855–858. 2011.
4. Ryu M, Kim EH, Chun M, Kang S, Shim B, Yu YB, Jeong G, and Lee JS. Astragali Radix elicits anti-inflammation via activation of MKP-1, concomitant with attenuation of p38 and Erk. J Ethnopharmacol. **115**: 184–193. 2008. [Medline] [CrossRef]
5. Zhu H, Zhang Y, Ye G, Li Z, Zhou P, and Huang C. In vivo and in vitro antiviral activities of calycosin-7-*O*-β-D-glucopyranoside against coxsackie virus B3. Biol Pharm Bull. **32**: 68–73. 2009. [Medline] [CrossRef]
6. Chan JYW, Lam FC, Leung PC, Che CT, and Fung KP. Antihyperglycemic and antioxidative effects of a herbal formulation of Radix Astragali, Radix Codonopsis and Cortex Lycii in a mouse model of type 2 diabetes mellitus. Phytother Res. **23**: 658–665. 2009. [Medline] [CrossRef]
7. Nalbantsoy A, Nesil T, Yılmaz-Dilsiz O, Aksu G, Khan S, and Bedir E. Evaluation of the immunomodulatory properties in mice and in vitro anti-inflammatory activity of cycloartane type saponins from Astragalus species. J Ethnopharmacol. **139**: 574–581. 2012. [Medline] [CrossRef]
8. [No authors listed]. Astragalus membranaceus. Monograph. Altern Med Rev. **8**: 72–77. 2003. [Medline]
9. Zhang G, Hu XJ, Jiang GZ, Liu YL, Ba XY. Identification of small molecular organic compounds of astragalus injection by LC/MC. Mod Chin Med. **18**: 410–414+430. 2016.
10. Wu JJ, Sun WY, Hu SS, Zhang S, and Wei W. A standardized extract from Paeonia lactiflora and Astragalus membranaceus induces apoptosis and inhibits the proliferation, migration and invasion of human hepatoma cell lines. Int J Oncol. **43**: 1643–1651. 2013. [Medline] [CrossRef]
11. OuYang Y, Huang J, OuYang Z, and Kang J. Enrichment and purification process of astragalosides and their anti-human gastric cancer MKN-74 cell proliferation effect. Afr Health Sci. **14**: 22–27. 2014. [Medline] [CrossRef]
12. Zhu J, Zhang H, Zhu Z, Zhang Q, Ma X, Cui Z, and Yao T. Effects and mechanism of flavonoids from Astragalus complanatus on breast cancer growth. Naunyn Schmiedebergs Arch Pharmacol. **388**: 965–972. 2015. [Medline] [CrossRef]
13. Tin MM, Cho CH, Chan K, James AE, and Ko JK. Astragalus saponins induce growth inhibition and apoptosis in human colon cancer cells and tumor xenograft. Carcinogenesis. **28**: 1347–1355. 2007. [Medline] [CrossRef]
14. Zhou RF, Liu PX, and Tan M. [Effect of Astragalus mongholicus injection on proliferation and apoptosis of hormone sensitive (MCF-7) breast cancer cell lines with physiological dose E2]. Zhong Yao Cai. **32**: 744–747. 2009; (in Chinese). [Medline]
15. Li X, Wang X, Han C, Wang X, Xing G, Zhou L, Li G, and Niu Y. Astragaloside IV suppresses collagen production of activated hepatic stellate cells via oxidative stress-mediated p38 MAPK pathway. Free Radic Biol Med. **60**: 168–176. 2013. [Medline] [CrossRef]
16. Hu YW, Liu CY, Du CM, Zhang J, Wu WQ, and Gu ZL. Induction of apoptosis in human hepatocarcinoma SMMC-7721 cells in vitro by flavonoids from Astragalus complanatus. J Ethnopharmacol. **123**: 293–301. 2009. [Medline] [CrossRef]
17. Wang P, Zhang Z, Sun Y, Liu X, and Tong T. The two isomers of HDTIC compounds from Astragali Radix slow

down telomere shortening rate via attenuating oxidative stress and increasing DNA repair ability in human fetal lung diploid fibroblast cells. DNA Cell Biol. **29**: 33–39. 2010. [Medline] [CrossRef]
18. Limagne E, Cottet V, Cotte AK, Hamza S, Hillon P, Latruffe N, Delmas D. CiRCE Study Group. Potential role of oxidative DNA damage in the impact of PNPLA3 variant (rs 738409 C>G) in hepatocellular carcinoma risk. Hepatology. **60**: 1110–1111. 2014. [Medline] [CrossRef]
19. Chen J, Wang G, Li L, and Zhang P. [Protective effect of Astragalus polysaccharide on MRC-5 cells from oxidative damage induced by hydrogen peroxide]. Xibao Yu Fenzi Mianyixue Zazhi. **31**: 1062–1066. 2015; (in Chinese). [Medline]
20. Imaida K, and Fukushima S. Initiation-promotion model for assessment of carcinogenicity: medium-term liver bioassay in rats for rapid detection of carcinogenic agents. J Toxicol Sci. **21**: 483–487. 1996. [Medline] [CrossRef]
21. Muguruma M, Kawai M, Dewa Y, Nishimura J, Saegusa Y, Yasuno H, Jin M, Matsumoto S, Takabatake M, Arai K, and Mitsumori K. Threshold dose of piperonyl butoxide that induces reactive oxygen species-mediated hepatocarcinogenesis in rats. Arch Toxicol. **83**: 183–193. 2009. [Medline] [CrossRef]
22. Shirai T. A medium-term rat liver bioassay as a rapid in vivo test for carcinogenic potential: a historical review of model development and summary of results from 291 tests. Toxicol Pathol. **25**: 453–460. 1997. [Medline] [CrossRef]
23. Ito N, Imaida K, Asamoto M, and Shirai T. Early detection of carcinogenic substances and modifiers in rats. Mutat Res. **462**: 209–217. 2000. [Medline] [CrossRef]
24. Livak KJ, and Schmittgen TD. Analysis of relative gene expression data using real-time quantitative PCR and the $2^{-\Delta\Delta C_T}$) Method. Methods. **25**: 402–408. 2001. [Medline] [CrossRef]
25. Hanahan D, and Weinberg RA. Hallmarks of cancer: the next generation. Cell. **144**: 646–674. 2011. [Medline] [CrossRef]
26. Hartwell LH, and Kastan MB. Cell cycle control and cancer. Science. **266**: 1821–1828. 1994. [Medline] [CrossRef]
27. Hassan M, Watari H, AbuAlmaaty A, Ohba Y, and Sakuragi N. Apoptosis and molecular targeting therapy in cancer. BioMed Res Int. **2014**: 150845. 2014. [Medline] [CrossRef]
28. Tong L, Chuang CC, Wu S, and Zuo L. Reactive oxygen species in redox cancer therapy. Cancer Lett. **367**: 18–25. 2015. [Medline] [CrossRef]
29. Huang WH, Liao WR, and Sun RX. Astragalus polysaccharide induces the apoptosis of human hepatocellular carcinoma cells by decreasing the expression of Notch1. Int J Mol Med. **38**: 551–557. 2016. [Medline] [CrossRef]
30. Lai X, Xia W, Wei J, and Ding X. Therapeutic effect of astragalus polysaccharides on hepatocellular carcinoma H22-bearing mice. Dose Response. **15**: 1559325816685182. 2017. [Medline] [CrossRef]
31. Qi L, Liu CY, Wu WQ, Gu ZL, and Guo CY. Protective effect of flavonoids from Astragalus complanatus on radiation induced damages in mice. Fitoterapia. **82**: 383–392. 2011. [Medline] [CrossRef]
32. Saleem S, Shaharyar MA, Khusroo MJ, Ahmad P, Rahman RU, Ahmad K, Alam MJ, Al-Harbi NO, Iqbal M, and Imam F. Anticancer potential of rhamnocitrin 4'-β-D-galactopyranoside against *N*-diethylnitrosamine-induced hepatocellular carcinoma in rats. Mol Cell Biochem. **384**: 147–153. 2013. [Medline] [CrossRef]
33. You N, Liu W, Wang T, Ji R, Wang X, Gong Z, Dou K, and Tao K. Swainsonine inhibits growth and potentiates the cytotoxic effect of paclitaxel in hepatocellular carcinoma in vitro and in vivo. Oncol Rep. **28**: 2091–2100. 2012. [Medline] [CrossRef]
34. Li YF, Han Y, Guo YL, Wang CJ, Li Y. Effects of Astragalus injection and aerobic exercise on Free Radical metabolism in heart and liver tissues of rats exhausted. J Guangxi Univ Chin Med. **14:** 3–5. 2011.
35. Wang L, Zheng L, Wang SY, Zhu TF, and Zhu HG. Clonal analysis of gastric carcinoma and precancerous lesions and its relation to Ki-67 protein expression. Neoplasma. **56**: 48–55. 2009. [Medline] [CrossRef]
36. Li LT, Jiang G, Chen Q, and Zheng JN. Ki67 is a promising molecular target in the diagnosis of cancer (review). Mol Med Rep. **11**: 1566–1572. 2015. [Medline] [CrossRef]
37. Maga G, and Hubscher U. Proliferating cell nuclear antigen (PCNA): a dancer with many partners. J Cell Sci. **116**: 3051–3060. 2003. [Medline] [CrossRef]
38. Gerdes J, Lemke H, Baisch H, Wacker HH, Schwab U, and Stein H. Cell cycle analysis of a cell proliferation-associated human nuclear antigen defined by the monoclonal antibody Ki-67. J Immunol. **133**: 1710–1715. 1984. [Medline]
39. Stoimenov I, and Helleday T. PCNA on the crossroad of cancer. Biochem Soc Trans. **37**: 605–613. 2009. [Medline] [CrossRef]
40. Wang SC. PCNA: a silent housekeeper or a potential therapeutic target? Trends Pharmacol Sci. **35**: 178–186. 2014. [Medline] [CrossRef]
41. Izutani Y, Yogosawa S, Sowa Y, and Sakai T. Brassinin induces G1 phase arrest through increase of p21 and p27 by inhibition of the phosphatidylinositol 3-kinase signaling pathway in human colon cancer cells. Int J Oncol. **40**: 816–824. 2012. [Medline]
42. Knudsen ES, and Zacksenhaus E. The vulnerability of RB loss in breast cancer: targeting a void in cell cycle control. Oncotarget. **9**: 30940–30941. 2018. [Medline] [CrossRef]
43. Knudsen ES, and Knudsen KE. Tailoring to RB: tumour suppressor status and therapeutic response. Nat Rev Cancer. **8**: 714–724. 2008. [Medline] [CrossRef]
44. Dulić V, Lees E, and Reed SI. Association of human cyclin E with a periodic G1-S phase protein kinase. Science. **257**: 1958–1961. 1992. [Medline] [CrossRef]
45. Frenzel A, Grespi F, Chmelewskij W, and Villunger A. Bcl2 family proteins in carcinogenesis and the treatment of cancer. Apoptosis. **14**: 584–596. 2009. [Medline] [CrossRef]
46. Ly JD, Grubb DR, and Lawen A. The mitochondrial membrane potential (deltapsi(m)) in apoptosis; an update. Apoptosis. **8**: 115–128. 2003. [Medline] [CrossRef]
47. Zhao Y, Lei M, Wang Z, Qiao G, Yang T, and Zhang J. TCR-induced, PKC-θ-mediated NF-κB activation is regulated by a caspase-8-caspase-9-caspase-3 cascade. Biochem Biophys Res Commun. **450**: 526–531. 2014. [Medline] [CrossRef]
48. Liu PF, Hu YC, Kang BH, Tseng YK, Wu PC, Liang CC, Hou YY, Fu TY, Liou HH, Hsieh IC, Ger LP, and Shu CW. Expression levels of cleaved caspase-3 and caspase-3 in tumorigenesis and prognosis of oral tongue squamous cell carcinoma. PLoS One. **12**: e0180620. 2017. [Medline] [CrossRef]